TOXICOLOGICAL SCIENCES **136(1)**, 131–143 2013
doi:10.1093/toxsci/kft179
Advance Access publication August 23, 2013

# Accumulated Polymer Degradation Products as Effector Molecules in Cytotoxicity of Polymeric Nanoparticles

Raman Preet Singh*[,2] and Poduri Ramarao*[,1,3]

*Department of Pharmacology and Toxicology, National Institute of Pharmaceutical Education and Research, S.A.S. Nagar, Punjab 160 062, India

[1]To whom correspondence should be addressed. Fax: +91-164-2430586. E-mail: ramaraop@yahoo.com.
[2]Present address: Evalueserve SEZ (Gurgaon) Pvt. Ltd, Sector 21, Gurgaon, Haryana 122 001, India.
[3]Present address: School of Basic and Applied Sciences, Central University of Punjab, Bathinda, Punjab 151 001, India.

Received April 11, 2013; accepted August 15, 2013

**Polymeric nanoparticles (PNPs) are a promising platform for drug, gene, and vaccine delivery. Although generally regarded as safe, the toxicity of PNPs is not well documented. The present study investigated *in vitro* toxicity of poly-ε-caprolactone, poly(DL-lactic acid), poly(lactide-cocaprolactone), and poly(lactide-co-glycide) NPs and possible mechanism of toxicity. The concentration-dependent effect of PNPs on cell viability was determined in a macrophage (RAW 264.7), hepatocyte (Hep G2), lung epithelial (A549), kidney epithelial (A498), and neuronal (Neuro 2A) cell lines. PNPs show toxicity at high concentrations in all cell lines. PNPs were efficiently internalized by RAW 264.7 cells and stimulated reactive oxygen species and tumor necrosis factor-alpha production. However, reactive nitrogen species and interleukin-6 production as well as lysosomal and mitochondrial stability remained unaffected. The intracellular degradation of PNPs was determined by monitoring changes in osmolality of culture medium and a novel fluorescence recovery after quenching assay. Cell death showed a good correlation with osmolality of culture medium suggesting the role of increased osmolality in cell death.**

***Key Words:*** **polymeric nanoparticles; *in vitro* toxicity; nanoparticle degradation; osmotic pressure; intracellular degradation; dye release; poly-ε-caprolactone; poly(DL-lactic acid); poly(lactide-cocaprolactone); poly(lactide-co-glycide)**

The recent surge in development of nanoparticle (NP)-based therapeutics has offered novel technologies for efficient delivery of drugs, genes, and vaccines (Shi *et al.*, 2010). The unique physicochemical properties of NPs offer the advantages of enhanced PO absorption, dose reduction, and reduced toxicity (Adair *et al.*, 2010; Mundargi *et al.*, 2008). These properties may be attributed to the enhanced cellular uptake of NPs. However, this enhanced cellular uptake can also lead to increased interaction of NPs with subcellular components resulting in stimulation of various signaling pathways. This elicits a stress response, which manifests as stimulation of free radical generation, organelle damage, and cell death (Bayles *et al.*, 2010; Wang *et al.*, 2011).

Several types of NPs are under investigation for delivery of therapeutic compounds including carbon nanotubes, metallic NPs, and polymeric NPs (PNPs). These delivery systems may be broadly divided into 2 categories: (1) those which require covalent linkage of molecules on surface and (2) those which require entrapment in the NP matrix. PNPs are versatile drug carriers and provide the ability to conjugate molecules on the NP surface as well as entrap molecules in NP matrix. Further, drug release profile, *in vivo* targeting, and bioavailability can be modulated by choosing appropriate polymers and by modifying polymer chemistry (Green *et al.*, 2008; Shi *et al.*, 2010). We have also shown that anticancer drug-encapsulated PNPs show higher bioavailability, higher pharmacological activity, and tumor targeting along with reduction in toxicity (Jain *et al.*, 2011a,b). The increased bioavailability of PNP-encapsulated drugs is due to higher intestinal absorption of NPs compared with free drug, whereas passive tumor targeting is achieved by enhanced permeation and retention effect (Jain *et al.*, 2011b).

The polymers employed in preparation of pharmaceutically relevant NPs have been used for a long time in tissue engineering and are generally regarded as safe (Kedar *et al.*, 2010). However, despite the fact that NPs behave differently from bulk materials, toxicity studies have not been reported in PNPs. It has been demonstrated that orally or systemically administered PNPs are predominantly distributed in reticuloendothelial system (hepatic and spleenic macrophages) apart from their ability to reach lungs and brain (Chang *et al.*, 2009; Ren *et al.*, 2009; Sivadas *et al.*, 2008; Swarnakar *et al.*, 2011). On the other hand, bulk polymer preparations induce only local responses at the site of administration (Kang *et al.*, 2007; Lickorish *et al.*, 2004).

We report the *in vitro* effects of PNPs of different chemical compositions on cell lines representing various target tissue compartments (macrophage, hepatocyte, renal epithelial, pulmonary epithelial, and neuronal cells). We report for the first time that accumulation of polymer degradation products results in PNP toxicity. Further, we also report a novel

fluorescence recovery after quenching (FRAQ) assay to determine intracellular degradation of PNPs.

## MATERIALS AND METHODS

***Chemicals.*** Coumarin 6, dialysis bags (cutoff 12 kDa), dichlorofluorescein diacetate (DCFDA), *Escherichia coli* O55:B5 lipopolysaccharide (LPS), 3-(4,5-dimethylthiazol-2-yl)-2,5-diphenyltetrazolium bromide (MTT), N-1-napthylethylenediamine dihydrochloride (NED), phosphoric acid, phorbol myristate acetate (PMA), polyvinyl alcohol (PVA; molecular weight 30 000–70 000), rhodamine 123 (Rh123), sodium nitrite, and Triton X-100 were obtained from Sigma, India. Dulbecco's Modified Eagle's medium (DMEM), fetal bovine serum (FBS), and antibiotics were purchased from PAA, Austria. Ethyl acetate and acetone were obtained from JT Baker, India. Poly(lactide-co-glycide) (PLGA), poly-ε-caprolactone (PCL), and poly(lactide-co-caprolactone) (PLCL) were obtained from Birmingham Polymers, United Kingdom, and included PLGA 50:50 (intrinsic viscosity 0.60 g/dl in hexafluoroisopropanol), PLGA 65:35 (intrinsic viscosity 0.64 g/dl in hexafluoroisopropanol), PLGA 75:25 (intrinsic viscosity 0.72 g/dl in chloroform), PLGA 85:15 (intrinsic viscosity 0.62 g/dl in chloroform), PCL (intrinsic viscosity 1.07 g/dl in chloroform), PLCL 25:75 (intrinsic viscosity 0.71 g/dl in chloroform), and PLCL 80:20 (intrinsic viscosity 0.77 g/dl in chloroform). Poly(DL-lactic acid) (DL-PLA; molecular weight 10 000) was obtained from Polysciences. Calcein acetoxymethyl ester (calcein-AM) was purchased from Calbiochem. Dimethylsulfoxide (DMSO) was obtained from Merck, India. Mouse tumor necrosis factor-α (TNF-α) and interleukin-6 (IL-6) enzyme-linked immunosorbent assay (ELISA) kits were purchased from eBioscience. All other chemicals used were of analytical grade.

***Preparation of blank PNPs.*** PLGA, DL-PLA, and PLCL PNPs were prepared by emulsion-diffusion-evaporation method, whereas PCL NPs were prepared by nanoprecipitation.

PNPs were prepared by emulsion-diffusion-evaporation method as described previously (Jain *et al.*, 2011a,b; Swarnakar *et al.*, 2011). Briefly, 50 mg polymer was dissolved in 2.5 ml ethyl acetate at room temperature and added dropwise into 5 ml of 2% wt/vol PVA solution under stirring at 1200 rpm. The stirring was continued for 30 min. The emulsion was homogenized at 15 000 rpm for 5 min. The resulting emulsion was diluted with 25 ml of 0.1% wt/vol PVA solution under magnetic stirring at 1200 rpm and stirred overnight to allow evaporation of organic solvent. The NP suspension was centrifuged at 20 000 × g for 15 min and the pellet was washed thrice with distilled water to remove free polymer and surfactant. The pellet was resuspended in 2.5 ml water.

PCL NPs were prepared by nanoprecipitation method as described elsewhere with minor modifications (Chawla and Amiji, 2002). Fifty milligrams of PCL was dissolved in 10 ml of acetone and added to 25 ml of 2% wt/vol PVA under magnetic stirring at 1200 rpm. This results in an opalescent liquid indicating formation of NPs. The NP suspension was centrifuged at 20 000 × g for 15 min and the pellet was washed thrice with 0.1% wt/vol PVA to remove free polymer. The pellet was resuspended in 2.5 ml of 0.1% PVA wt/vol to prevent NP aggregation.

***Preparation of Coumarin 6-loaded PNPs.*** Coumarin 6-loaded PNPs were prepared for determining cellular uptake of NPs (Jain *et al.*, 2011a; Panyam *et al.*, 2003; Swarnakar *et al.*, 2011). The dye was dissolved in organic phase (100 µg/50 mg polymer) and PNPs were prepared as described for blank PNPs above.

**In vitro *release of Coumarin 6.*** One milliliter of Coumarin 6-loaded PNP suspension (10 mg/ml), prepared in PBS (pH 7.4), was loaded in dialysis bags. The dialysis bag was immersed in 10 ml PBS and incubated at 37°C in shaking water bath at 50 rpm. One milliliter aliquots were removed after 3-, 6-, 12-, and 24-h incubation. The released dye was determined fluorimetrically at excitation wavelength of 458 nm and emission wavelength of 505 nm (Jain *et al.*, 2011a; Panyam *et al.*, 2003).

***Preparation of calcein-AM-loaded PNPs.*** Calcein-AM was dissolved in organic phase (50 µg/50 mg polymer) and NPs were prepared by nanoprecipitation as described for blank PCL NPs.

***Characterization of PNPs.*** The average diameter, size distribution, polydispersity index (PDI), and zeta potential of PNPs (1–5 mg/ml) were determined by dynamic light scattering (DLS) using Zeta Sizer (Malvern, United Kingdom). The morphology of NPs was determined by Veeco BioScope II atomic force microscope (AFM). Briefly, a small drop of PNP suspension (approximately 50 µl; 10 mg/ml) was placed on a silicon wafer and air-dried. Tapping mode measurements were recorded using a FESP cantilever (length = 325 µm, width = 26 µm, tip diameter = 117 nm) (Chavanpatil *et al.*, 2006; Mittal *et al.*, 2007; Swarnakar *et al.*, 2011).

***Cells.*** The macrophage (RAW 264.7), hepatocyte (Hep G2), renal epithelial (A498), pulmonary epithelial (A549), and neuronal (Neuro 2A) cell lines were obtained from National Centre for Cell Sciences, Pune, India. The cells were grown in tissue culture flasks in DMEM supplemented with 10% FBS and antibiotics. Confluent cultures of cells were trypsinized and seeded in 96-well tissue culture plates as described earlier (Jain *et al.*, 2011a; Swarnakar *et al.*, 2011). Cells were incubated overnight for attachment in wells and medium was replaced with fresh culture medium containing NPs.

***Cytotoxicity studies.*** Cells ($1 \times 10^4$/well) were incubated with various concentrations of NPs for 72 h. After incubation, cells were washed up to 5 times with PBS to remove NPs and cell viability was determined by MTT and Coomassie blue (CB) assay as described earlier (Singh *et al.*, 2012; Singh and Ramarao, 2012). Briefly, culture supernatants from control or NP-containing wells were collected and cells incubated with MTT (0.5 mg/ml; 3 h). The formazon was dissolved in 200 µl DMSO and optical density measured at 550 nm. For CB assay, the culture supernatants were collected and 200 µl of Bradford reagent was added to each well. The reaction was allowed to proceed for 30 min and absorbance was determined at 595 nm. The absorbance of control wells was assumed 100% and cell viability of treated wells was determined with respect to control wells.

***Free radical and cytokine production.*** Free radical production was determined by monitoring production of reactive oxygen species (ROS) and reactive nitrogen species (RNS) in RAW 264.7 cells. RAW 264.7 cells ($1 \times 10^5$/well) were incubated with NP-containing medium for 24 h and culture supernatants were collected. Cells were washed 5 times with PBS to remove extracellular NPs and ROS production was determined by DCFDA assay as described earlier (Singh and Ramarao, 2012). PMA (10 µg/ml) was included as positive control.

RNS production was determined by nitrite assay in culture supernatants using Griess reagent (Tsikas, 2005). Griess reagent was prepared by mixing equal volumes of solution A (prepared by dissolving 1 g sulfanilamide in 100 ml of 5% phosphoric acid) and solution B (prepared by dissolving 100 mg NED in 100 ml water). Equal volumes of culture supernatant and Griess reagent (100 µl each) were mixed and kept at room temperature for 30 min. This results in formation of a diazo salt with maximum absorption at 540 nm. The nitrite concentration was calculated from standard plot constructed using sodium nitrite as standard (Singh *et al.*, 2012; Singh and Ramarao, 2012).

TNF-α and IL-6 levels were assayed in culture supernatants by colorimetric ELISA kits as per manufacturer's instructions. LPS (10 µg/ml) was included as positive control for nitrite and cytokine production.

***Mitochondrial stability assay.*** Changes in mitochondrial membrane potential (MMP) were determined by Rh123 and Safranin O (SafO) assays. RAW 264.7 cells were incubated with NPs for 24 h, washed with PBS, and incubated with Rh123 (10 µg/ml, 30 min) (Singh and Ramarao, 2012) or SafO (10 µg/ml, 30 min). Cells were again washed with PBS to remove excess dye. Rh123 fluorescence intensity was determined at 530 nm excitation and 590 nm emission. The absorbance of SafO was determined at 523 and 555 nm and the ratio of intensities was calculated (Deryabina *et al.*, 2001; Severin *et al.*, 2010). Sodium azide ($10^{-2}$ M added 30 min before recording) was included as positive control (Johnson *et al.*, 1981).

***Lysosomal stability assay.*** Lysosomal stability was determined by leakage of acridine orange (AO) from AO-loaded lysosomes and accumulation of neutral red (NR) in intact lysosomes. Lead (50 µM) was included as positive control (Bussolaro *et al.*, 2008).

AO is a lysomotropic agent, which preferentially accumulates in lysosomes and exhibits red fluorescence in lysosomes. However, when lysosomes are damaged, AO leaks out into the cytoplasm and gives a green fluorescence. The intensity of green fluorescence increases with an increase in lysosomal damage. Further, the increase in green fluorescence (due to cytoplasmic AO) appears early compared with reduction in red fluorescence (due to lysosomal AO) (Antunes *et al.*, 2001; Castino *et al.*, 2007). RAW 264.7 cells ($1 \times 10^5$/well) were loaded with 5 μg/ml AO for 15 min. The excess dye was removed by washing with PBS and cells were incubated with NP-containing medium for 8 h. The cells were again washed 5 times with PBS to remove extracellular NPs and fluorescence intensity was determined at 488 nm excitation and 540 nm emission.

NR assay is based on the accumulation of the dye in intact lysosomes. A reduction in viable lysosomes leads to reduction in NR uptake by cells. RAW 264.7 cells were incubated with NPs for 24 h, washed with PBS, and incubated with NR (50 μg/ml in culture medium) for 2 h. The dye was then removed and cells were washed thrice with PBS. The intracellular dye was dissolved in 100 μl acid alcohol (1% acetic acid in 50% ethanol) and absorbance determined at 540 nm.

***Cellular uptake of PNPs.*** The cellular uptake of PNPs was determined fluorimetrically using Coumarin 6-loaded NPs (Panyam *et al.*, 2003). For qualitative cell uptake studies, RAW 264.7 cells were incubated with 100 μg/ml Coumarin 6-loaded PNPs for 3 h and cellular uptake was observed by confocal microscopy. To determine the quantitative uptake of NPs, Coumarin 6-labeled NPs were incubated with RAW 264.7 cells ($1 \times 10^5$ cells/well) for various time intervals (1–12 h) and then washed 5 times with PBS to remove extracellular NPs. Cells were then lysed with 200 μl water containing 0.1% vol/vol Triton X-100 and fluorescence intensity of cell lysate was determined at 458 nm excitation and 505 nm emission.

***Biodegradation of PNPs.*** The biodegradability of PNPs was determined by monitoring changes in osmolality of culture medium and by release of calcein-AM from PNPs.

PNP suspension was added to culture medium to achieve final concentrations of 10, 30, 100, 300, and 1000 μg/ml, and 200 μl of various concentrations of PNPs was incubated with RAW 264.7 cells ($1 \times 10^4$ cells/well) at 37°C. After 72-h incubation, the pH and osmolality were determined. Osmolality measurements were performed using a vapor pressure osmometer (Vapro 5520, Wescor, Inc) according to manufacturer's recommendations. Briefly, 20 μl of sample was loaded on a filter paper disc and inserted in the instrument. The instrument provides osmolality in millimoles per kilogram. pH measurements were performed using a pH meter. Culture medium without PNPs (0 μg/ml PNP) was included as control to monitor changes in osmolality and pH due to cellular metabolism and evaporation of culture medium.

pH and osmolality were determined by 2 protocols. In the first protocol, culture medium was centrifuged (20 000 × g, 15 min) to separate PNPs and pH and osmolality of supernatant were determined (Cordewener *et al.*, 2000). In the second protocol, pH and osmolality of culture medium were determined directly, without removal of PNPs by centrifugation. The pH and osmolality determined by the 2 protocols were similar indicating the presence of PNPs does not interfere with estimation of pH and osmolality.

RAW 264.7 cells ($1 \times 10^4$/well) were incubated with 200 μl of calcein-AM-loaded PNPs (100 μg/ml) for 3 h. The extracellular NPs were removed by 5 washes with PBS and further incubated for 72 h. Following incubation, the cells were observed under confocal microscope at 488 nm excitation to determine biodegradability of PNPs. The intracellular release of calcein was also determined fluorimetrically at 488 nm excitation and 515 nm emission following cell lysis after 72 h as described above.

***Statistical analysis.*** All values are expressed as mean ± SEM. Treatment groups were compared by 1-way ANOVA followed by Tukey's test and $p < .05$ was considered significant.

## RESULTS AND DISCUSSION

A wide range of polymers are currently under investigation as vehicles for delivery of therapeutic molecules. PLGA is the most commonly employed polymer due to its high biocompatibility and the ability to modulate drug release by careful selection of lactide/glycide monomer ratios. Further, PLA, PCL, and copolymers with varying ratios of lactide/caprolactone (PLCL) are also under investigation due to their high drug loading capacity and composition-dependent polymer degradation and drug release behavior (Dinarvand *et al.*, 2011; Kamel *et al.*, 2009; Seyednejad *et al.*, 2011; Uskokovic and Stevanovic, 2009). Therefore, considering the effect of composition on polymer degradation behavior, 4 types of PLGA and 2 types of PLCL with different monomer ratios were selected for this study. Additionally, homopolymers PLA and PCL were also studied.

### *PNP Characterization*

PNPs were characterized by AFM (Fig. 1) and DLS (Table 1). AFM revealed that PNPs were spherical in shape and around 200 nm in size with narrow size distribution. Average particle size of PNPs observed by DLS was in close agreement with AFM results. Further, zeta potential measurements showed that PNPs carried a small negative charge of around −10 mV. The size and zeta potential were similar (± 5%) when measurements were performed in water (Table 1) or culture medium containing serum (data not shown) as shown previously (Harde *et al.*, 2013). Further, DLS measurements showed no signs of PNP agglomeration after 72 h of incubation in culture medium as hydrodynamic diameter of PNPs was similar (± 10%) at 0 h and after 72 h (data not shown).

### *Cytotoxicity of PNPs*

Our group has been extensively involved in developing PNP-based therapeutics for delivery of anticancer drugs. We observed that passive targeting to liver and spleen represents the major mechanism for systemic clearance of PNPs. Further, cellular uptake of NPs by RAW 264.7 cells provides a reliable alternate to predict *in vivo* uptake of NPs by reticuloendothelial system (Harde *et al.*, 2013). Based on studies with drug-loaded PNPs conducted by our group, we assumed that a nominal dose of 10 mg/kg drug will be delivered in 100 mg/kg of PNPs, assuming 10% drug loading in PNPs. Based on our previous study on *in vitro* toxicity of carbon NPs (Singh *et al.*, 2012), we calculated that an *in vivo* dose of 100 mg will correspond to approximately 150 μg/ml PNPs in RAW 264.7 cell culture. Hence, a concentration higher by one order of magnitude (1000 μg/ml) was selected as the highest concentration.

RAW 264.7 cells were incubated with PNPs for 24, 48, and 72 h, and cell viability was determined by MTT and CB assay. PNPs showed no change in cell viability up to 48 h of incubation at all concentrations (data not shown) and up to a concentration of 100 μg/ml after 72-h incubation. A further increase in concentration to 300 and 1000 μg/ml resulted in a concentration-dependent reduction in cell viability after 72-h incubation. The results of MTT and CB assay after 72-h incubation are shown in Figure 2 and Supplementary Figure S1,

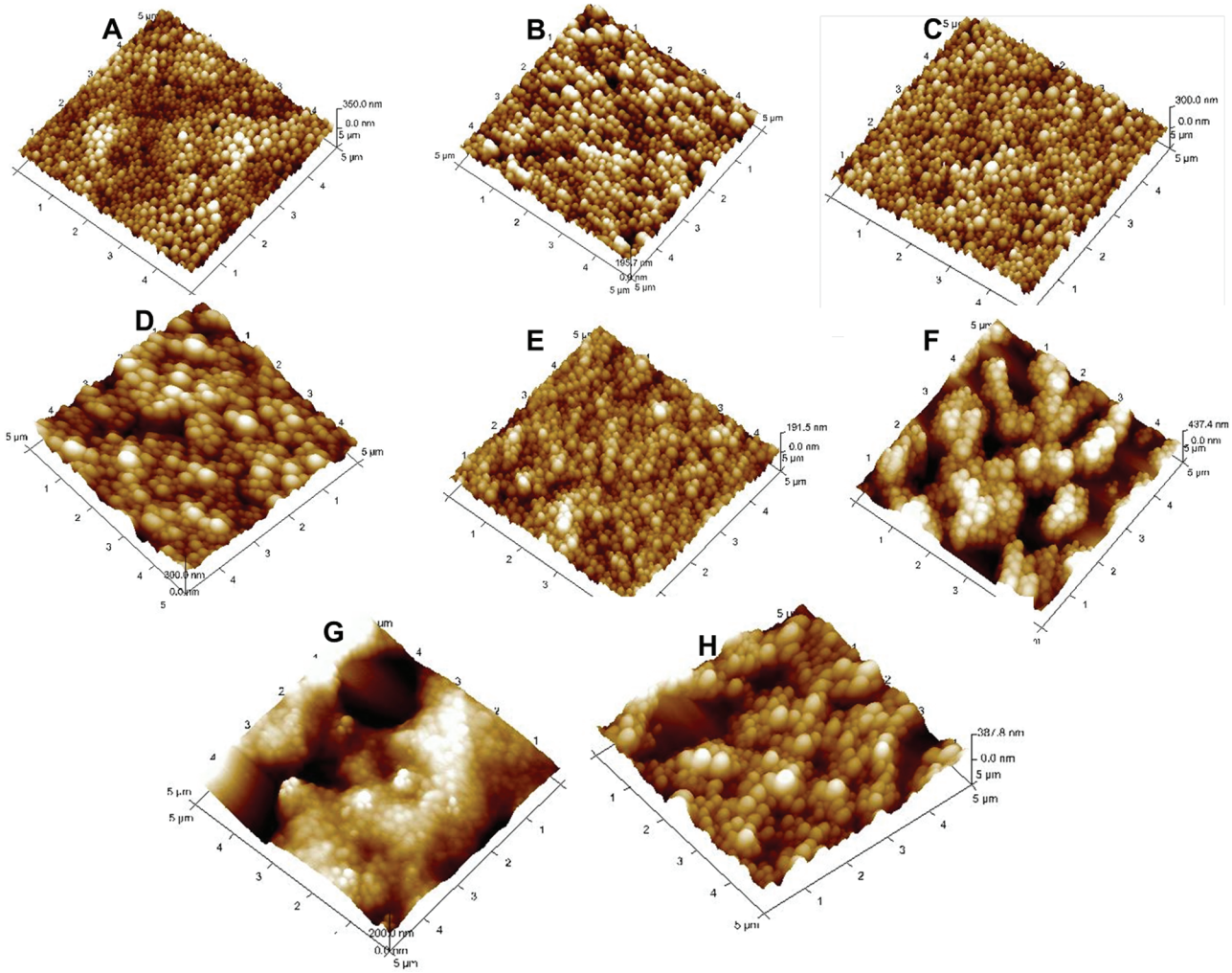


**FIG. 1.** AFM images of PLGA 50:50 (A), PLGA 65:35 (B), PLGA 75:25 (C), PLGA 85:15 (D), DL-PLA (E), PCL (F), PLCL 25:75 (G), and PLCL 80:20 (H) NPs. Abbreviations: AFM, atomic force microscope; DL-PLA, poly(DL-lactic acid); NPs, nanoparticles; PCL, poly-ε-caprolactone; PLCL, poly(lactide-co-caprolactone); PLGA, poly(lactide-co-glycide).

respectively. Similar results were observed in other cell lines and after 72-h incubation with PNPs (Supplementary Figures S2–S9). Macrophages (RAW 264.7) were found to be slightly more sensitive to PNP-induced cytotoxicity compared with other cell types. The general order of susceptibility was found to be RAW 264.7 ≥ A549 > Hep G2 > A498 > Neuro 2A. This is in agreement with higher sensitivity of macrophages to carbon nanotube-induced cytotoxicity (Sohaebuddin *et al.*, 2010).

*Cellular Uptake of PNPs*

It has been demonstrated that the cytotoxicity of NPs is dependent on their cellular uptake (Geys *et al.*, 2008; Ryman-Rasmussen *et al.*, 2007). It may be argued that the low toxicity of PNPs may be due to their inefficient cellular uptake. To rule out this possibility, cellular uptake of fluorescent (Coumarin 6) PNPs was determined. The DLS characteristics of Coumarin 6-loaded PNPs were similar to blank PNPs (Table 2). *In vitro* release of Coumarin 6 from PNPs showed that less than 1% dye leached from PNPs in 24 h (Supplementary Figure S10).

**TABLE 1**
**Particle Characteristics of PNPs Determined by DLS**

| Polymer Type | Average Diameter (nm) | PDI | Zeta Potential (mV) |
|---|---|---|---|
| PLGA 50:50 | 257 | 0.053 | −8.0 |
| PLGA 65:35 | 234 | 0.014 | −9.9 |
| PLGA 75:25 | 295 | 0.059 | −12.3 |
| PLGA 85:15 | 252 | 0.012 | −10.5 |
| DL-PLA | 288 | 0.079 | −11.9 |
| PCL | 363 | 0.039 | −8.2 |
| PLCL 25:75 | 228 | 0.037 | −12.6 |
| PLCL 80:20 | 241 | 0.049 | −10.2 |

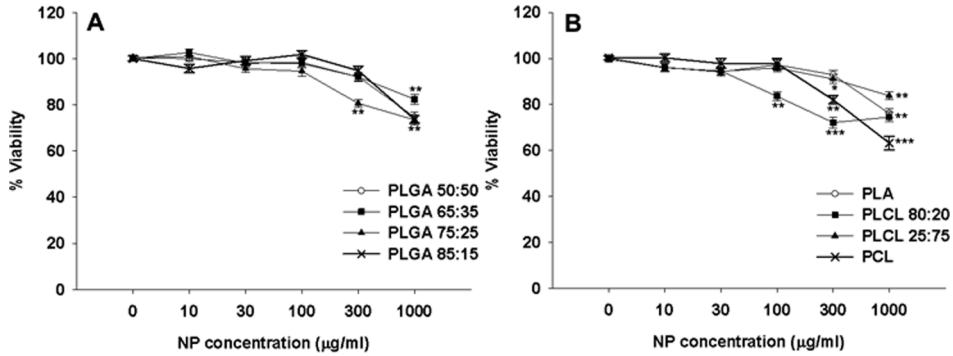


**FIG. 2.** Effect of PNPs on cell viability after 72-h incubation with RAW 264.7 cells ($n$ = 15/concentration). *$p$ < .05, **$p$ < .01, ***$p$ < .001 with respect to control. Abbreviations: NP, nanoparticle; PCL, poly-ε-caprolactone; PLA, poly(DL-lactic acid); PLCL, poly(lactide-co-caprolactone); PLGA, poly(lactide-co-glycide); PNPs, polymeric NPs.

**TABLE 2**
**Particle Characteristics of Coumarin 6-Loaded PNPs**

| Polymer Type | Size (nm) | PDI | Zeta Potential (mV) |
|---|---|---|---|
| PLGA 50:50 | 210 | 0.030 | −14.0 |
| PLGA 65:35 | 211 | 0.015 | −8.70 |
| PLGA 75:25 | 218 | 0.153 | −12.7 |
| PLGA 85:15 | 243 | 0.127 | −12.7 |
| DL-PLA | 256 | 0.028 | −17.1 |
| PCL | 268 | 0.033 | −9.10 |
| PLCL 25:75 | 261 | 0.122 | −15.3 |
| PLCL 80:20 | 261 | 0.021 | −15.4 |

Confocal microscopy revealed that PNPs are effectively internalized after 3-h incubation with RAW 264.7 cells (Fig. 3). The NPs appeared to be present in cytoplasmic compartment and did not enter cell nucleus. However, 2-dimensional imaging cannot effectively differentiate between intracellular and surface-bound PNPs. Thus, 3-dimensional imaging was performed by Z-sectioning followed by 3-dimensional reconstruction to confirm the cellular uptake of PNPs. Three-dimensional reconstructed images confirmed that PNPs were present in the cytoplasmic compartment and excluded by cell nucleus. The cytoplasmic fluorescence was mainly diffused along with occasional punctuate appearance. Although the punctuate fluorescence indicates that the PNPs are localized in cellular organelles (eg, lysosomes), the diffused cytoplasmic fluorescence indicates that PNPs are present in the cytoplasm. It has been suggested that PLGA NPs may be trafficked to the lysosomal compartment where they may undergo charge reversal resulting in lysosomal escape (Cartiera *et al.*, 2009; Panyam *et al.*, 2002). Thus, the NPs may be present in cell organelles as well as in cytoplasm.

*Stress Responses Induced by PNPs*

The confocal microscopy results suggest that PNPs may interact with cytoplasmic components and induce a stress response. Among the various stress responses elicited by NPs, free radical generation and inflammation appear the earliest and were studied in macrophages (RAW 264.7 cells) for 2 reasons. First, majority of the PNPs administered *in vivo* are internalized by macrophages of reticoendothelial system. Second, free radical and cytokine production is the highest in macrophages.

The concentration-dependent effect of PNPs on free radical production was determined. Stimulation of ROS production was determined after 24-h incubation of cells with PNPs using the fluorescent probe, DCFDA. PNPs showed no effect on ROS production up to 100 μg/ml concentration, whereas 300 μg/ml showed 1.5- to 2-fold stimulation of ROS production (Fig. 4). A further increase in PNP concentration to 1000 μg/ml interfered with ROS assay due to fluorescence quenching. The positive control (PMA) resulted in 3.5- to 4-fold increase in ROS production compared with basal levels. In contrast to stimulation of ROS production, PNPs did not stimulate RNS in macrophages up to the highest concentration (1000 μg/ml) of PNPs (data not shown), whereas the positive control (LPS) resulted in over 2-fold increase in nitrite level compared with control. Similarly, PNPs did not stimulate the release of IL-6 at 300 μg/ml although a 1.5- to 2-fold increase in TNF-α release was observed at 300 μg/ml PNPs (Fig. 5). The positive control (LPS) stimulated production of both cytokines in macrophages resulting in approximately 10-fold increase in IL-6 levels and 8-fold increase in TNF-α levels compared with untreated control.

PNPs stimulated ROS and TNF-α production at high concentrations only, whereas RNS and IL-6 production remained unaffected. These results suggest that ROS and TNF-α production are more sensitive to PNP exposure compared with RNS and IL-6 and the former may be useful tools in detecting potential toxic/inflammatory effects of NPs. Similar results showing macrophage stimulation and enhanced ROS production have been reported in bulk polymers (Gil *et al.*, 2010; Jain *et al.*, 2011a), and in implants, grafts and scaffolds (Allen *et al.*, 2005; Charrois and Allen, 2004) and microspheres (Lim *et al.*, 1997, 2000; Xiong *et al.*, 2010) prepared using PLGA, PCL, and DL-PLA.

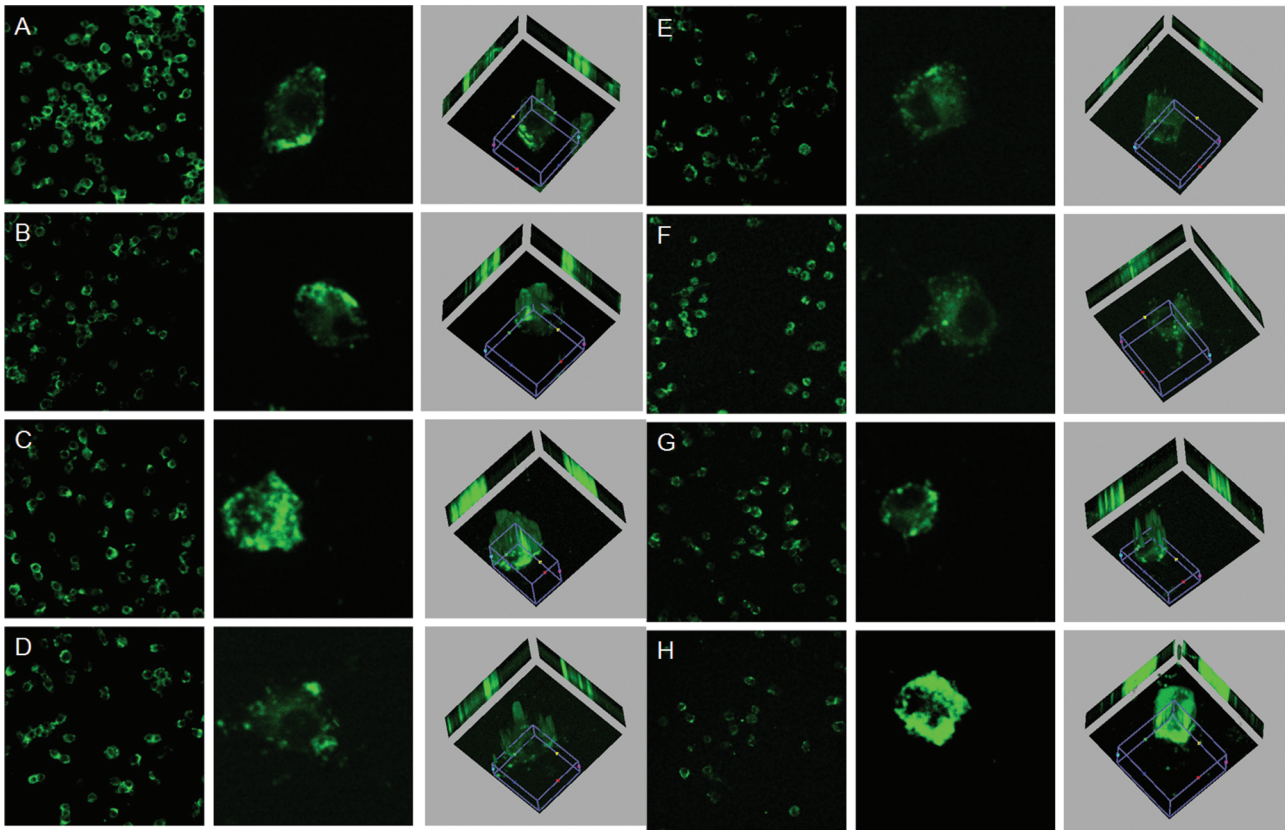


**FIG. 3.** Confocal microscopy images showing cellular uptake of PNPs. The images show uptake of PLGA 50:50 (A), PLGA 65:35 (B), PLGA 75:25 (C), PLGA 85:15 (D), DL-PLA (E), PCL (F), PLCL 25:75 (G), and PLCL 80:20 (H) NPs in RAW 264.7 cells. The left panel shows a low magnification image, and the middle panel shows a magnified image of a single cell with internalized PNPs. The right panel is the 3-dimensional image (Z-sectioning and 3D reconstruction) of the cell shown in middle panel. Abbreviations: DL-PLA, poly(DL-lactic acid); NPs, nanoparticles; PCL, poly-ε-caprolactone; PLCL, poly(lactide-co-caprolactone); PLGA, poly(lactide-co-glycide); PNPs, polymeric NPs.

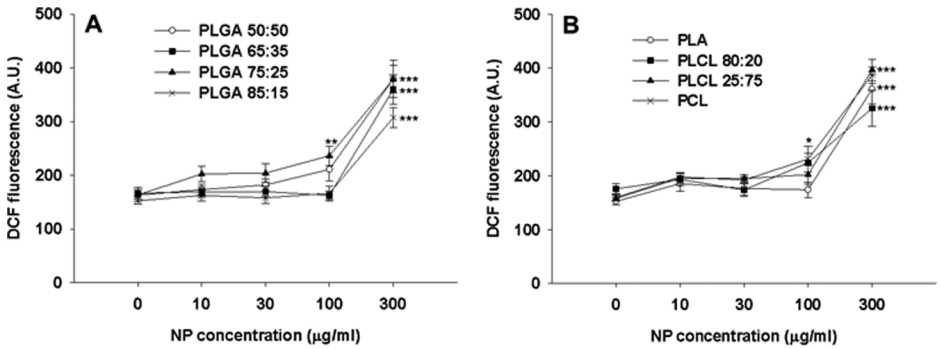


**FIG. 4.** Effect of PNPs on ROS production after 24-h incubation with RAW 264.7 cells ($n$ = 5–10/concentration). *$p$ < .05, **$p$ < .01, ***$p$ < .001 with respect to control. Abbreviations: DCF, dichlorofluorescein; NP, nanoparticle; PCL, poly-ε-caprolactone; PLA, poly(DL-lactic acid); PLCL, poly(lactide-co-caprolactone); PLGA, poly(lactide-co-glycide); PNPs, polymeric NPs; ROS, reactive oxygen species.

It has been suggested that NPs are trafficked to mitochondria and lysosomes (Bayles *et al.*, 2010; Cartiera *et al.*, 2009; Panyam *et al.*, 2002; Wang *et al.*, 2011). Thus, internalization of NPs can also lead to destabilization of cellular organelles. Such destabilization may arise through induction of oxidative stress (Daiber, 2010; Terman *et al.*, 2010; Weber and Reichert, 2010) or by direct interaction of NPs with cellular organelles. Mitochondrial and lysosomal damage has been reported in several types of NPs including carbon nanotubes and metallic NPs (Sohaebuddin *et al.*, 2010; Teodoro *et al.*, 2011; Zhong *et al.*, 2010). The changes in lysosomal and mitochondrial integrity are early events in induction of cell death and can be detected within few hours of exposure to toxicants (Daiber, 2010; Das *et al.*, 2013; Singh *et al.*, 2012; Terman *et al.*, 2010). Therefore,

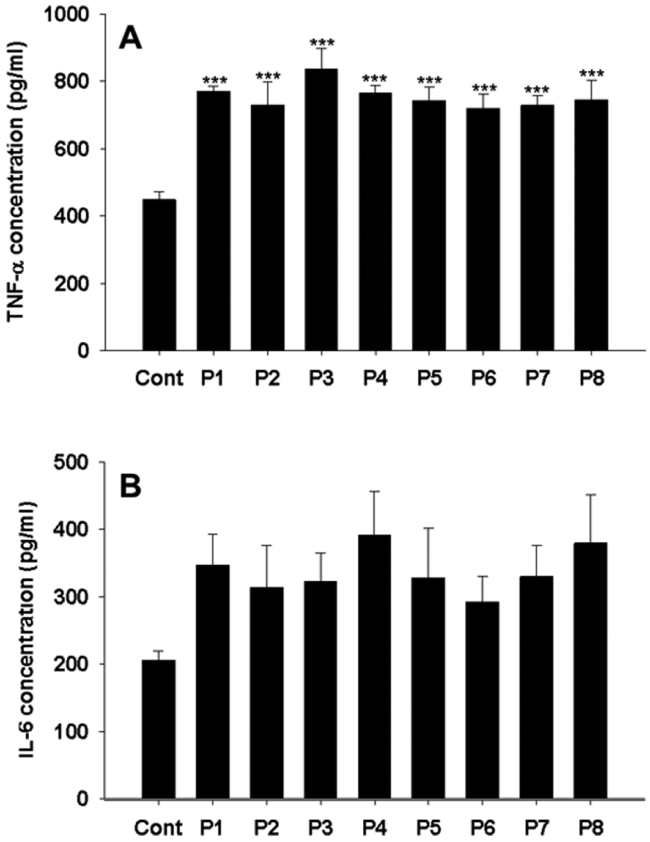


**FIG. 5.** Effect of PLGA 50:50 (P1), PLGA 65:35 (P2), PLGA 75:25 (P3), PLGA 85:15 (P4), DL-PLA (P5), PCL (P6), PLCL 25:75 (P7), and PLCL 80:20 (P8) NPs on cytokine release after 24-h incubation with RAW 264.7 cells ($n$ = 3–4 for each PNP type). ***$p < .001$ with respect to control. Abbreviations: DL-PLA, poly(DL-lactic acid); IL-6, interleukin-6; NPs, nanoparticles; PCL, poly-ε-caprolactone; PLCL, poly(lactide-co-caprolactone); PLGA, poly(lactide-co-glycide); PNP, polymeric NP; TNF-α, tumor necrosis factor-α.

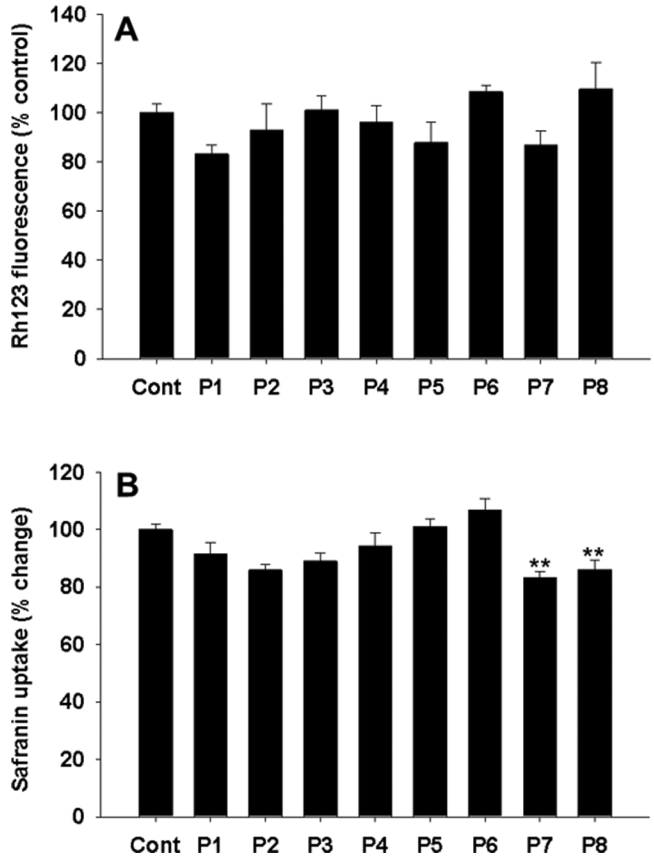


**FIG. 6.** Effect of PLGA 50:50 (P1), PLGA 65:35 (P2), PLGA 75:25 (P3), PLGA 85:15 (P4), DL-PLA (P5), PCL (P6), PLCL 25:75 (P7), and PLCL 80:20 (P8) NPs on mitochondria after 24-h incubation with RAW 264.7 cells ($n$ = 5–10 for each PNP type). **$p < .01$ with respect to control. Abbreviations: DL-PLA, poly(DL-lactic acid); NPs, nanoparticles; PCL, poly-ε-caprolactone; PLCL, poly(lactide-co-caprolactone); PLGA, poly(lactide-co-glycide); PNP, polymeric NP; Rh123, rhodamine 123.

mitochondrial and lysosomal stability was assessed by colorimetric and fluorimetric methods. Further, 300 μg/ml PNP concentration was chosen for assay of organelle stability because lower concentrations were nontoxic, whereas higher concentrations lead to fluorescence quenching. The fluorescence intensity of Rh123 and the 523/555 nm ratio of SafO are directly related to MMP. A decrease in fluorescence intensity (Rh123) or 523/555 nm ratio (SafO) corresponds to a reduction in MMP. We observed that none of the PNPs showed a significant reduction in MMP (Fig. 6). On the other hand, MMP was reduced to approximately 70% and 50% as determined Rh123 and SafO methods, respectively, following treatment with positive control (sodium azide). Although PLCL 25:75 and PLCL 80:20 NPs showed reduction in MMP in SafO assay, but no effect was observed in Rh123 assay. However, differences in cell viability determined by assays based on metabolic activity (MTT and CB assay) suggest the possibility of mitochondrial damage at higher PNP concentrations (Singh and Ramarao, 2012). Further, no change in lysosomal integrity was observed in AO and NR assays. The AO fluorescence intensity in control and PNP-treated (300 μg/ml) RAW 264.7 cells was similar after 8-h incubation. Additionally, NR uptake was similar in control and PNP-treated (300 μg/ml) cells after 24-h incubation (Fig. 7). The positive control caused approximately 50% increase in AO relocalization and approximately 50% reduction in NR uptake following treatment with positive control (lead).

The above results suggest that PNPs are generally tolerated by cells and no significant effects on free radical generation, cytokine production, mitochondria, and lysosomes are observed. Thus, the observed reduction in cell viability may be attributed to mechanism(s) other than stimulation of free radical generation or organelle damage. It is known that PNPs are biodegradable in nature and their biodegradation is an important factor determining the release of entrapped therapeutic compounds. It has been demonstrated that polymeric implants show inflammation and cytotoxicity due to accumulation of low-molecular-weight polymer degradation products (Kang *et al.*, 2007; Lickorish *et al.*, 2004). Therefore,

we investigated the role of polymer degradation products in PNP toxicity.

*Polymer Degradation*

Several approaches are available to determine degradation of PNPs including gel permeation chromatography (Barbosa *et al.*, 2003), nuclear magnetic resonance (Barbosa *et al.*, 2003), Raman spectroscopy (Chernenko *et al.*, 2009), release of a fluorescent compound, and changes in osmolality and pH (Cordewener *et al.*, 2000). However, nearly all these methods suffer from limitations. The sample requirements for gel permeation chromatography and nuclear magnetic resonance are of the order of a few milligrams. It is practically not feasible to apply these methods for estimation of intracellular NP degradation because cellular biomolecules adsorbed on NP surface may interfere with estimation of polymer molecular weight. Raman spectroscopy of cells is a useful tool in determining intracellular degradation of NPs. However, the Raman signal for polymers suffers from interference by cellular lipids, eg, endoplasmic reticulum and lysosome membranes (Chernenko *et al.*, 2009). The release of a fluorescent dye cannot be used to measure the intracellular degradation because extracellular NPs may also degrade in the culture medium. The determination of pH is a sensitive parameter for measuring polymer degradation. However, changes in pH may not be suitable because culture medium is a buffered solution and can control changes in pH. Polymer degradation leads to generation of smaller polymer fragments of lower molecular weight. This leads to an increase in the number of molecules in solution. Because osmotic pressure is a colligative property (and depends on total number of molecules), polymer degradation to smaller fragments increases the osmolality of solution (Cordewener *et al.*, 2000).

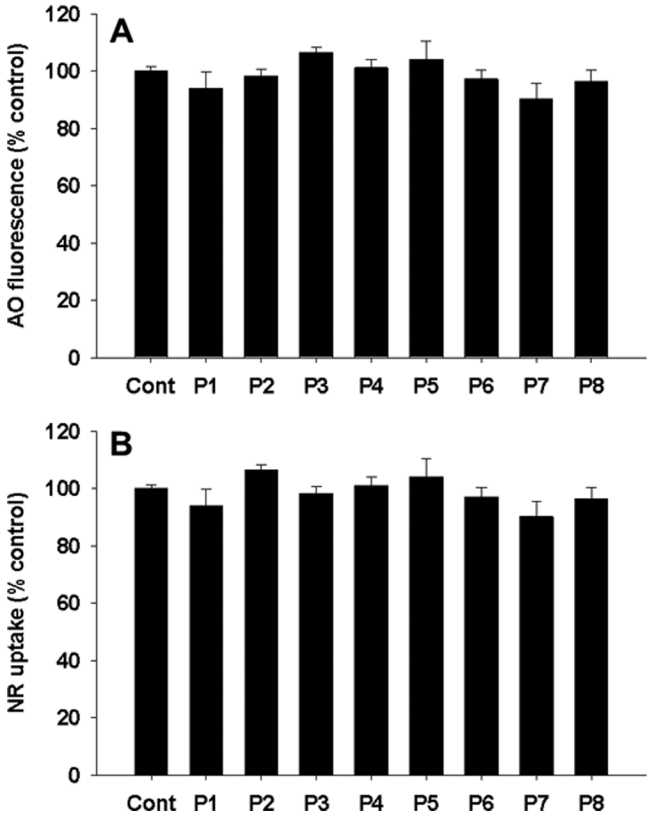


**FIG. 7.** Effect of PLGA 50:50 (P1), PLGA 65:35 (P2), PLGA 75:25 (P3), PLGA 85:15 (P4), DL-PLA (P5), PCL (P6), PLCL 25:75 (P7), and PLCL 80:20 (P8) NPs on lysosomes after 24-h incubation with RAW 264.7 cells ($n$ = 5–10 for each PNP type). Abbreviations: AO, acridine orange; DL-PLA, poly(DL-lactic acid); NPs, nanoparticles; NR, neutral red; PCL, poly-ε-caprolactone; PLCL, poly(lactide-co-caprolactone); PLGA, poly(lactide-co-glycide); PNP, polymeric NP.

The addition of PNPs to culture medium showed no change in osmolality or pH (at 0 h) up to the highest concentration (1000 µg/ml). However, a concentration-dependent increase in osmotic pressure was observed at 100 µg/ml and higher concentrations after 72-h incubation of PNPs with RAW 264.7 cells (Fig. 8). Further, a PNP-free control was included to account for changes in medium osmolality due to cellular metabolism and/or evaporation of medium. An increase in osmolality by 2%–5% (typically < 10 mmol/kg) of the basal values was observed during the course of experiment. We believe that such small changes in osmolality due to cellular metabolism are biologically insignificant and do not impact the outcome of the

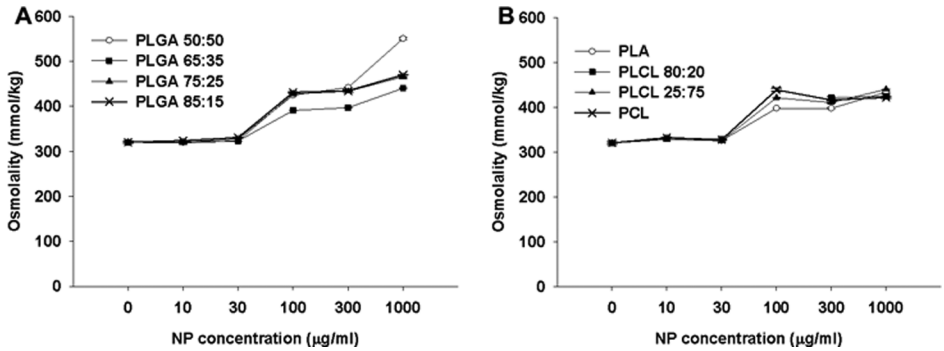


**FIG. 8.** Osmolality of PNP suspensions after 72-h incubation with RAW 264.7 cells ($n$ = 3–6/concentration). Abbreviations: NP, nanoparticle; PLA, poly(DL-lactic acid); PCL, poly-ε-caprolactone; PLCL, poly(lactide-co-caprolactone); PLGA, poly(lactide-co-glycide); PNP, polymeric NP.

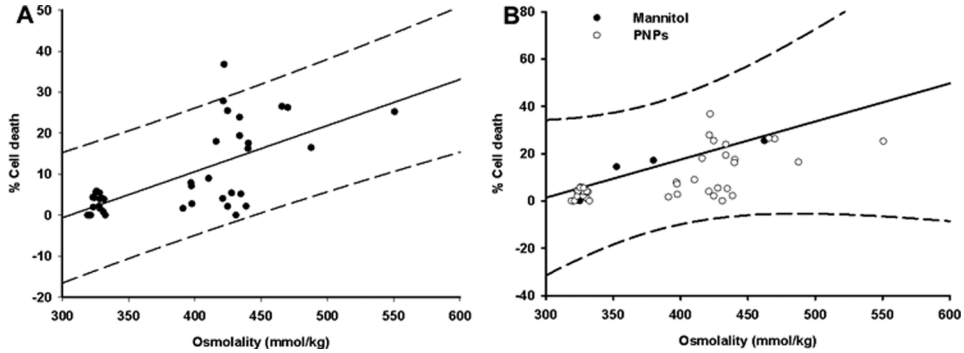


**FIG. 9.** Correlation between osmolality and cell death determined by MTT assay (A) and fitting of data in osmolality-cell death correlation of mannitol (B). Abbreviations: MTT, 3-(4,5-dimethylthiazol-2-yl)-2,5-diphenyltetrazolium bromide; PNPs, polymeric nanoparticles.

present study. Contrastingly, pH of culture medium remained unchanged (data not shown) due to buffering capacity of the culture medium. Thus, study of changes in osmolality seemed to be the most viable methodology and indicate that degradation of PNPs can be studied by monitoring changes in osmotic pressure at PNP concentrations as low as 100 µg/ml and in very small sample volumes (20 µl). Such sensitivity is not achieved in other methods of polymer degradation.

As observed in Figures 2 and 8, the increase in osmolality was associated with an increase in cell death. Thus, we hypothesized that the increase in osmolality may lead to cell death. Regression analysis showed that a linear correlation exists between osmolality and cell death observed with PNPs (Fig. 9A). To validate this hypothesis, mannitol was used to increase osmolality of the culture medium. Mannitol is an inert compound, and toxicity of mannitol may be attributed to an increase in osmotic pressure only. Regression analysis showed that a linear correlation exists between osmolality and cell death for mannitol (Fig. 9B). When data points of PNPs were fitted in osmolality-cell death correlation of mannitol, all data points were observed to lie within 95% confidence interval. Thus, it may be inferred that accumulation of polymer degradation products leads to an increase in osmolality, which, in turn, leads to cell death. In order to segregate the contribution of PNPs and polymer degradation products in cell death, culture medium was replaced regularly (every 24 h) during incubation period (72 h). This regular replacement of culture medium ensures removal of polymer degradation products while PNPs remained in contact with cells. The toxicity, thus observed, may be attributed to PNPs only. After 72-h incubation with PNPs with regular culture medium replacement, no cell death was observed (data not shown). The absence of PNP-induced cytotoxicity with regular culture medium replacement suggests that PNPs are nontoxic and underscores the role of polymer degradation products in PNP-induced cell death.

The intracellular degradation of PNPs was also evaluated by a novel FRAQ assay. Calcein gives green fluorescence in aqueous medium and its fluorescence can be quenched by acetylation. The acetylated product (calcein-AM) can be converted back to calcein by esterase-mediated enzymatic hydrolysis. Calcein is hydrophilic in nature and cannot easily cross the cell membrane resulting in intracellular accumulation of the fluorescent compound (calcein). Calcein-AM-loaded PNPs were prepared by nanoprecipitation method in contrast to emulsion-diffusion-evaporation method used for blank and Coumarin 6-loaded PNPs due to low dye loading efficiency in the later method. The mean particle size of calcein-AM-loaded PNPs was higher than blank PNPs (Table 3) because NPs prepared by nanoprecipitation yield particles of relatively higher particle size. However, zeta potential remained unchanged.

**TABLE 3**
**Particle Characteristics of Calcein-AM-Loaded PNPs**

| Polymer Type | Size (nm) | PDI | Zeta Potential (mV) |
|---|---|---|---|
| PLGA 50:50 | 331.8 | 0.175 | −11.2 |
| PLGA 65:35 | 338.8 | 0.117 | −10.5 |
| PLGA 75:25 | 434.5 | 0.293 | −10.2 |
| PLGA 85:15 | 407.7 | 0.231 | −7.96 |
| DL-PLA | 366.5 | 0.143 | −12.1 |
| PCL | 448.7 | 0.233 | −8.92 |
| PLCL 25:75 | 395.2 | 0.118 | −9.09 |
| PLCL 80:20 | 389.4 | 0.263 | −8.44 |

In order to differentiate between calcein-AM released from intracellular and extracellular NPs, it was necessary to "load" the cells with nonfluorescent NPs and remove the extracellular NPs. The uptake of NPs is concentration- and time-dependent in nature, and the optimal conditions for cellular uptake were determined. Quantitative cellular uptake studies using Coumarin 6-loaded PNPs showed that cellular uptake reached saturation at 100 µg/ml PNPs between 3- and 6-h incubation. Thus, cells were incubated with 100 µg/ml calcein-AM-loaded PNPs for 3 h followed by 5 washings with PBS to obtain calcein-AM PNP-loaded cells. After 72-h incubation, green fluorescence (from calcein) was observed microscopically indicating that NPs have degraded intracellularly and released the dye (Figs. 10A–H). Further,

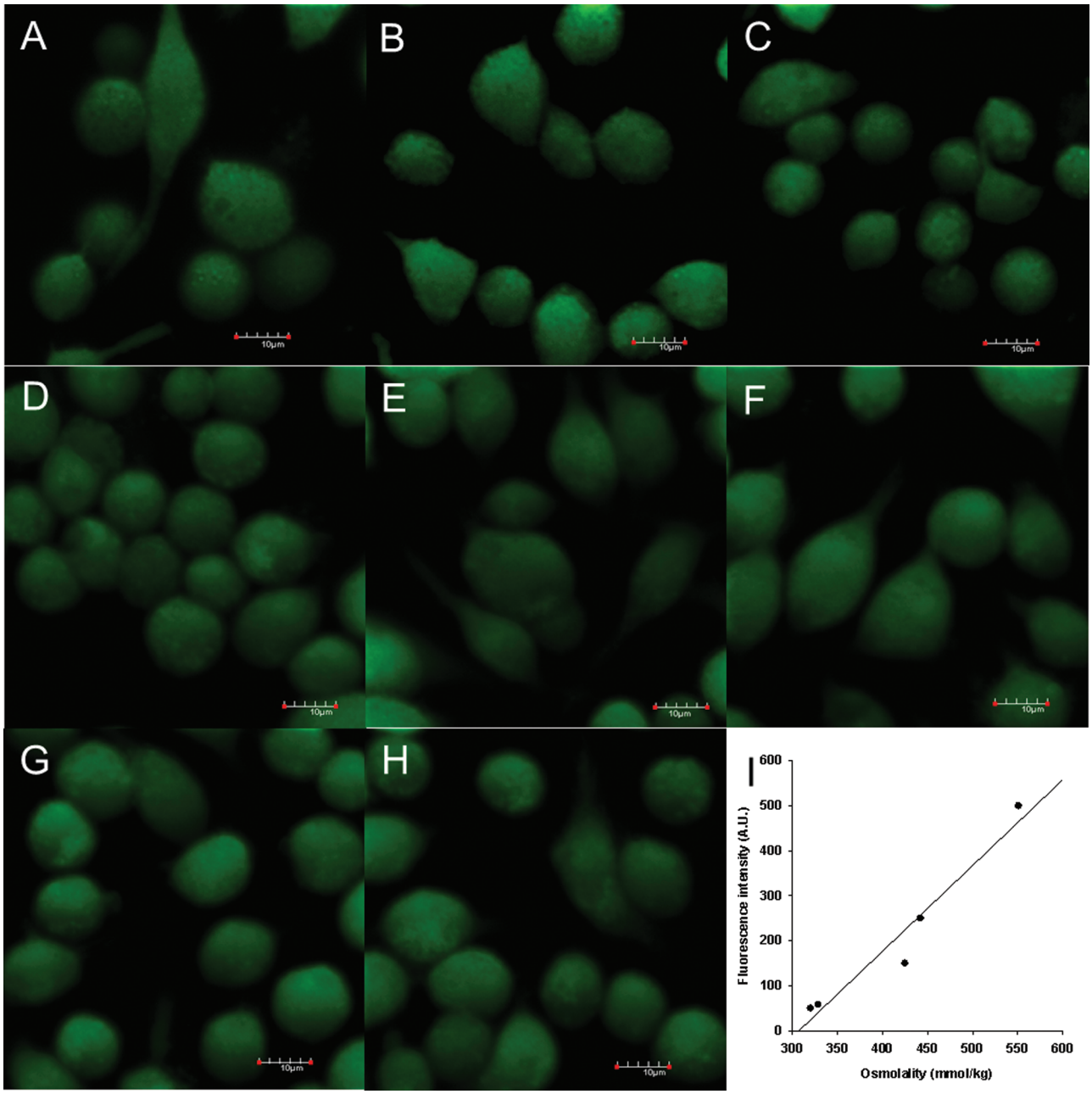


**FIG. 10.** Intracellular degradation of calcein-AM-loaded PLGA 50:50 (A), PLGA 65:35 (B), PLGA 75:25 (C), PLGA 85:15 (D), DL-PLA (E), PCL (F), PLCL 25:75 (G), and PLCL 80:20 (H) NPs in RAW 264.7 cells. (I) Correlation between calcein release from PLGA 50:50 NPs and osmolality of culture medium. Abbreviations: calcein-AM, calcein acetoxymethyl ester; DL-PLA, poly(DL-lactic acid); NPs, nanoparticles; PCL, poly-ε-caprolactone; PLCL, poly(lactide-co-caprolactone); PLGA, poly(lactide-co-glycide).

the release of calcein from PLGA 50:50 NPs showed a good correlation ($R = 0.971$) with osmolality (Fig. 10I). Similarly, increase in calcein fluorescence correlated with osmotic pressure ($R > 0.9$) in other PNPs as well (data not shown) indicating that calcein-AM release is due to degradation of PNPs and not leeching out from PNPs. We suggest that this approach can be extended to other polymers as well to determine intracellular degradation of NPs.

The effect of hyperosmolarity on cellular physiology and pathology has been reported in *in vitro* and *in vivo* systems. Several studies suggest that increased osmolality can trigger an inflammatory response, possibly by activating stress-related genes resulting in increased production of inflammatory cytokines (Brocker *et al.*, 2012; Lee *et al.*, 2008; Luo *et al.*, 2007; Schwartz *et al.*, 2009). Further, hyperosmolarity can also induce increased free radical production and activate apoptotic

cell death mechanisms (Kultz, 2004; Lee *et al.*, 2008; Luo *et al.*, 2007), affect mitochondrial and DNA integrity (Brocker *et al.*, 2012), and increase sensitivity to chemical-induced toxicity (Clouzeau *et al.*, 2012). We believe that the observed cytotoxicity and stress responses induced by PNPs are a result of increased osmolality due to degradation of polymer. This further supported by observations that cytotoxicity has a direct correlation with osmolality of the culture medium. Further, removal of polymer degradation products by replacement of culture medium abrogated cytotoxicity of PNPs suggesting the involvement of accumulated polymer degradation products (or increased osmolality) in induction of stress responses while the PNPs are, *per se*, biocompatible even at very high concentrations.

The results of the present study provide experimental evidence for biocompatibility of a large number of PNPs of different chemical compositions. PNPs are efficiently internalized by macrophages and did not induce untoward effects on RNS and IL-6 production or mitochondrial and lysosomal integrity. However, PNPs stimulate ROS and TNF-α production at high concentrations. PNPs degrade to low molecular polymer chains and may show cytotoxicity due to accumulation of polymer degradation products (Fig. 11). A novel FRAQ assay is described, which correlates with osmolality data. The assay can be considered a platform technology to determine intracellular degradation of a wide range of NPs.

It may be argued that, under *in vivo* conditions, the degradation products may be eliminated by excretion or enter into metabolic reaction cycles (eg, lactate may enter citric acid pathway) and PNPs may be well tolerated. *In vivo* studies with PNPs from our group and others have also reported the biocompatibility of PNPs (Forrest and Kwon, 2008; Jain *et al.*, 2011a; Prencipe *et al.*, 2009). However, possibility exists that PNPs may induce an inflammatory response if the polymer degradation products are not cleared from the site of administration similar to that observed in implants and grafts (Cao *et al.*, 2010; Kim *et al.*, 2007).

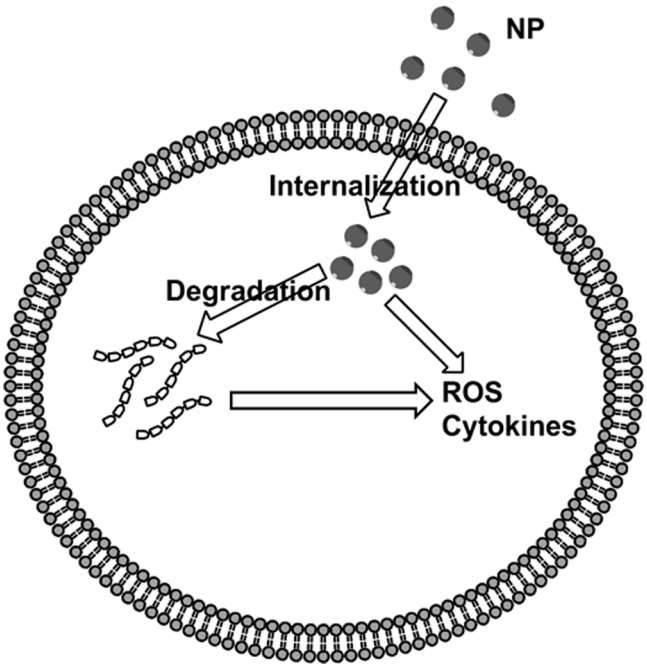


**FIG. 11.** Mechanism of cytotoxicity of PNPs. Abbreviations: NP, nanoparticle; PNPs, polymeric nanoparticles; ROS, reactive oxygen species.

## SUPPLEMENTARY DATA

Supplementary data are available online at http://toxsci.oxfordjournals.org/.

## FUNDING

Department of Science and Technology; Department of Pharmaceuticals, Government of India.

## ACKNOWLEDGMENTS

R.P.S. received Senior Research Fellowship from DST. We thank Dr Vijender Singh Beniwal for technical help in AFM characterization. The authors declare no conflict of interest.

## REFERENCES

Adair, J. H., Parette, M. P., Altinoğlu, E. I., and Kester, M. (2010). Nanoparticulate alternatives for drug delivery. *ACS Nano* **4,** 4967–4970.

Allen, T. M., Mumbengegwi, D. R., and Charrois, G. J. (2005). Anti-CD19-targeted liposomal doxorubicin improves the therapeutic efficacy in murine B-cell lymphoma and ameliorates the toxicity of liposomes with varying drug release rates. *Clin. Cancer Res*. **11,** 3567–3573.

Antunes, F., Cadenas, E., and Brunk, U. T. (2001). Apoptosis induced by exposure to a low steady-state concentration of H2O2 is a consequence of lysosomal rupture. *Biochem. J*. **356**(Pt 2), 549–555.

Barbosa, M. E. M., Cammas, S., Appel, M., and Ponchel, G. (2003). Investigation of the degradation mechanisms of poly(malic acid) esters in vitro and their related cytotoxicities on J774 macrophages. *Biomacromolecules* **5,** 137–143.

Bayles, A. R., Chahal, H. S., Chahal, D. S., Goldbeck, C. P., Cohen, B. E., and Helms, B. A. (2010). Rapid cytosolic delivery of luminescent nanocrystals in live cells with endosome-disrupting polymer colloids. *Nano Lett*. **10,** 4086–4092.

Brocker, C., Thompson, D. C., and Vasiliou, V. (2012). The role of hyperosmotic stress in inflammation and disease. *Biomol. Concepts* **3,** 345–364.

Bussolaro, D., Filipak Neto, F., Gargioni, R., Fernandes, L. C., Randi, M. A., Pelletier, E., and Oliveira Ribeiro, C. A. (2008). The immune response of peritoneal macrophages due to exposure to inorganic lead in the house mouse Mus musculus. *Toxicol. In Vitro* **22,** 254–260.

Cao, H., McHugh, K., Chew, S. Y., and Anderson, J. M. (2010). The topographical effect of electrospun nanofibrous scaffolds on the in vivo and in vitro foreign body reaction. *J. Biomed. Mater. Res. A* **93,** 1151–1159.

Cartiera, M. S., Johnson, K. M., Rajendran, V., Caplan, M. J., and Saltzman, W. M. (2009). The uptake and intracellular fate of PLGA nanoparticles in epithelial cells. *Biomaterials* **30,** 2790–2798.

Castino, R., Bellio, N., Nicotra, G., Follo, C., Trincheri, N. F., and Isidoro, C. (2007). Cathepsin D-Bax death pathway in oxidative stressed neuroblastoma cells. *Free Radic. Biol. Med*. **42,** 1305–1316.

Chang, J., Jallouli, Y., Kroubi, M., Yuan, X. B., Feng, W., Kang, C. S., Pu, P. Y., and Betbeder, D. (2009). Characterization of endocytosis of transferrin-coated PLGA nanoparticles by the blood-brain barrier. *Int. J. Pharm*. **379,** 285–292.

Charrois, G. J., and Allen, T. M. (2004). Drug release rate influences the pharmacokinetics, biodistribution, therapeutic activity, and toxicity of pegylated liposomal doxorubicin formulations in murine breast cancer. *Biochim. Biophys. Acta* **1663,** 167–177.

Chavanpatil, M. D., Patil, Y., and Panyam, J. (2006). Susceptibility of nanoparticle-encapsulated paclitaxel to P-glycoprotein-mediated drug efflux. *Int. J. Pharm*. **320,** 150–156.

Chawla, J. S., and Amiji, M. M. (2002). Biodegradable poly(epsilon -caprolactone) nanoparticles for tumor-targeted delivery of tamoxifen. *Int. J. Pharm*. **249,** 127–138.

Chernenko, T., Matthäus, C., Milane, L., Quintero, L., Amiji, M., and Diem, M. (2009). Label-free Raman spectral imaging of intracellular delivery and degradation of polymeric nanoparticle systems. *ACS Nano* **3,** 3552–3559.

Clouzeau, C., Godefroy, D., Riancho, L., Rostène, W., Baudouin, C., and Brignole-Baudouin, F. (2012). Hyperosmolarity potentiates toxic effects of benzalkonium chloride on conjunctival epithelial cells in vitro. *Mol. Vis*. **18,** 851–863.

Cordewener, F. W., van Geffen, M. F., Joziasse, C. A. P., Schmitz, J. P., Bos, R. R. M., Rozema, F. R., and Pennings, A. J. (2000). Cytotoxicity of poly(96L/4D-lactide): The influence of degradation and sterilization. *Biomaterials* **21,** 2433–2442.

Daiber, A. (2010). Redox signaling (cross-talk) from and to mitochondria involves mitochondrial pores and reactive oxygen species. *Biochim. Biophys. Acta* **1797,** 897–906.

Das, M., Singh, R. P., Datir, S. R., and Jain, S. (2013). Surface chemistry dependent "switch" regulates the trafficking and therapeutic performance of drug-loaded carbon nanotubes. *Bioconjug. Chem*. **24,** 626–639.

Deryabina, Y. I., Bazhenova, E. N., Saris, N. E., and Zvyagilskaya, R. A. (2001). Ca(2+) efflux in mitochondria from the yeast *Endomyces magnusii*. *J. Biol. Chem*. **276,** 47801–47806.

Dinarvand, R., Sepehri, N., Manoochehri, S., Rouhani, H., and Atyabi, F. (2011). Polylactide-co-glycolide nanoparticles for controlled delivery of anticancer agents. *Int. J. Nanomedicine* **6,** 877–895.

Forrest, M. L., and Kwon, G. S. (2008). Clinical developments in drug delivery nanotechnology. *Adv. Drug Deliv. Rev*. **60,** 861–862.

Geys, J., Nemmar, A., Verbeken, E., Smolders, E., Ratoi, M., Hoylaerts, M. F., Nemery, B., and Hoet, P. H. (2008). Acute toxicity and prothrombotic effects of quantum dots: Impact of surface charge. *Environ. Health Perspect*. **116,** 1607–1613.

Gil, P. R., Oberdörster, G., Elder, A., Puntes, V., and Parak, W. J. (2010). Correlating physico-chemical with toxicological properties of nanoparticles: The present and the future. *ACS Nano* **4,** 5527–5531.

Green, J. J., Zhou, B. Y., Mitalipova, M. M., Beard, C., Langer, R., Jaenisch, R., and Anderson, D. G. (2008). Nanoparticles for gene transfer to human embryonic stem cell colonies. *Nano Lett*. **8,** 3126–3130.

Harde, H., Singh, R. P., Agrawal, A. K., and Jain, S. (2013). Disease-based selection of nanocarriers in drug delivery based on hydrophobicity and surface charge. *J. Nanogenomics Nanomedicine* (forthcoming).

Jain, A. K., Swarnakar, N. K., Godugu, C., Singh, R. P., and Jain, S. (2011a). The effect of the oral administration of polymeric nanoparticles on the efficacy and toxicity of tamoxifen. *Biomaterials* **32,** 503–515.

Jain, A. K., Swarnakar, N. K., Godugu, C., Singh, R. P., Ramarao, P., and Jain, S. (2011b). Augmented anticancer efficacy of doxorubicin-loaded polymeric nanoparticles after oral administration in a breast cancer induced animal model. *Mol. Pharm*. **8,** 1140–1151.

Johnson, L. V., Walsh, M. L., Bockus, B. J., and Chen, L. B. (1981). Monitoring of relative mitochondrial membrane potential in living cells by fluorescence microscopy. *J. Cell Biol*. **88,** 526–535.

Kamel, A. O., Awad, G. A., Geneidi, A. S., and Mortada, N. D. (2009). Preparation of intravenous stealthy acyclovir nanoparticles with increased mean residence time. *AAPS PharmSciTech* **10,** 1427–1436.

Kang, S. W., Cho, E. R., Jeon, O., and Kim, B. S. (2007). The effect of microsphere degradation rate on the efficacy of polymeric microspheres as bulking agents: An 18-month follow-up study. *J. Biomed. Mater. Res. B Appl. Biomater*. **80,** 253–259.

Kedar, U., Phutane, P., Shidhaye, S., and Kadam, V. (2010). Advances in polymeric micelles for drug delivery and tumor targeting. *Nanomedicine* **6,** 714–729.

Kim, M. S., Ahn, H. H., Shin, Y. N., Cho, M. H., Khang, G., and Lee, H. B. (2007). An in vivo study of the host tissue response to subcutaneous implantation of PLGA- and/or porcine small intestinal submucosa-based scaffolds. *Biomaterials* **28,** 5137–5143.

Kultz, D. (2004). Hyperosmolality triggers oxidative damage in kidney cells. *Proc. Natl. Acad. Sci. U.S.A*. **101,** 9177–9178.

Lee, J. H., Kim, M., Im, Y. S., Choi, W., Byeon, S. H., and Lee, H. K. (2008). NFAT5 induction and its role in hyperosmolar stressed human limbal epithelial cells. *Invest. Ophthalmol. Vis. Sci*. **49,** 1827–1835.

Lickorish, D., Chan, J., Song, J., and Davies, J. E. (2004). An in-vivo model to interrogate the transition from acute to chronic inflammation. *Eur. Cell. Mater*. **8,** 12–19.

Lim, H. J., Masin, D., Madden, T. D., and Bally, M. B. (1997). Influence of drug release characteristics on the therapeutic activity of liposomal mitoxantrone. *J. Pharmacol. Exp. Ther*. **281,** 566–573.

Lim, H. J., Masin, D., McIntosh, N. L., Madden, T. D., and Bally, M. B. (2000). Role of drug release and liposome-mediated drug delivery in governing the therapeutic activity of liposomal mitoxantrone used to treat human A431 and LS180 solid tumors. *J. Pharmacol. Exp. Ther*. **292,** 337–345.

Luo, L., Li, D. Q., and Pflugfelder, S. C. (2007). Hyperosmolarity-induced apoptosis in human corneal epithelial cells is mediated by cytochrome c and MAPK pathways. *Cornea* **26,** 452–460.

Mittal, G., Sahana, D. K., Bhardwaj, V., and Kumar, M. N. V. R. (2007). Estradiol loaded PLGA nanoparticles for oral administration: Effect of polymer molecular weight and copolymer composition on release behavior in vitro and in vivo. *J. Control. Release* **119,** 77–85.

Mundargi, R. C., Babu, V. R., Rangaswamy, V., Patel, P., and Aminabhavi, T. M. (2008). Nano/micro technologies for delivering macromolecular therapeutics using poly(D,L-lactide-co-glycolide) and its derivatives. *J. Control. Release* **125,** 193–209.

Panyam, J., Sahoo, S. K., Prabha, S., Bargar, T., and Labhasetwar, V. (2003). Fluorescence and electron microscopy probes for cellular and tissue uptake of poly(D,L-lactide-co-glycolide) nanoparticles. *Int. J. Pharm*. **262,** 1–11.

Panyam, J., Zhou, W. Z., Prabha, S., Sahoo, S. K., and Labhasetwar, V. (2002). Rapid endo-lysosomal escape of poly(DL-lactide-co-glycolide) nanoparticles: Implications for drug and gene delivery. *FASEB J*. **16,** 1217–1226.

Prencipe, G., Tabakman, S. M., Welsher, K., Liu, Z., Goodwin, A. P., Zhang, L., Henry, J., and Dai, H. (2009). PEG branched polymer for functionalization of nanomaterials with ultralong blood circulation. *J. Am. Chem. Soc*. **131,** 4783–4787.

Ren, T., Xu, N., Cao, C., Yuan, W., Yu, X., Chen, J., and Ren, J. (2009). Preparation and therapeutic efficacy of polysorbate-80-coated amphotericin B/PLA-b-PEG nanoparticles. *J. Biomater. Sci. Polym. Ed*. **20,** 1369–1380.

Ryman-Rasmussen, J. P., Riviere, J. E., and Monteiro-Riviere, N. A. (2007). Variables influencing interactions of untargeted quantum dot nanoparticles

with skin cells and identification of biochemical modulators. *Nano Lett*. **7,** 1344–1348.

Schwartz, L., Guais, A., Pooya, M., and Abolhassani, M. (2009). Is inflammation a consequence of extracellular hyperosmolarity? *J. Inflamm. (Lond)*. **6,** 21.

Severin, F. F., Severina, I. I., Antonenko, Y. N., Rokitskaya, T. I., Cherepanov, D. A., Mokhova, E. N., Vyssokikh, M. Y., Pustovidko, A. V., Markova, O. V., Yaguzhinsky, L. S., *et al.* (2010). Penetrating cation/fatty acid anion pair as a mitochondria-targeted protonophore. *Proc. Natl. Acad. Sci. U.S.A*. **107,** 663–668.

Seyednejad, H., Ghassemi, A. H., van Nostrum, C. F., Vermonden, T., and Hennink, W. E. (2011). Functional aliphatic polyesters for biomedical and pharmaceutical applications. *J. Control. Release* **152,** 168–176.

Shi, J., Votruba, A. R., Farokhzad, O. C., and Langer, R. (2010). Nanotechnology in drug delivery and tissue engineering: From discovery to applications. *Nano Lett*. **10,** 3223–3230.

Singh, R. P., Das, M., Thakare, V., and Jain, S. (2012). Functionalization density dependent toxicity of oxidized multiwalled carbon nanotubes in a murine macrophage cell line. *Chem. Res. Toxicol*. **25,** 2127–2137.

Singh, R. P., and Ramarao, P. (2012). Cellular uptake, intracellular trafficking and cytotoxicity of silver nanoparticles. *Toxicol. Lett*. **213,** 249–259.

Sivadas, N., O'Rourke, D., Tobin, A., Buckley, V., Ramtoola, Z., Kelly, J. G., Hickey, A. J., and Cryan, S. A. (2008). A comparative study of a range of polymeric microspheres as potential carriers for the inhalation of proteins. *Int. J. Pharm*. **358,** 159–167.

Sohaebuddin, S. K., Thevenot, P. T., Baker, D., Eaton, J. W., and Tang, L. (2010). Nanomaterial cytotoxicity is composition, size, and cell type dependent. *Part. Fibre Toxicol*. **7,** 22.

Swarnakar, N. K., Jain, A. K., Singh, R. P., Godugu, C., Das, M., and Jain, S. (2011). Oral bioavailability, therapeutic efficacy and reactive oxygen species scavenging properties of coenzyme Q10-loaded polymeric nanoparticles. *Biomaterials* **32,** 6860–6874.

Teodoro, J. S., Simões, A. M., Duarte, F. V., Rolo, A. P., Murdoch, R. C., Hussain, S. M., and Palmeira, C. M. (2011). Assessment of the toxicity of silver nanoparticles in vitro: A mitochondrial perspective. *Toxicol. In Vitro* **25,** 664–670.

Terman, A., Kurz, T., Navratil, M., Arriaga, E. A., and Brunk, U. T. (2010). Mitochondrial turnover and aging of long-lived postmitotic cells: The mitochondrial-lysosomal axis theory of aging. *Antioxid. Redox Signal*. **12,** 503–535.

Tsikas, D. (2005). Methods of quantitative analysis of the nitric oxide metabolites nitrite and nitrate in human biological fluids. *Free Radic. Res*. **39,** 797–815.

Uskokovic, D., and Stevanovic, M. (2009). Poly(lactide-co-glycolide)-based micro and nanoparticles for the controlled drug delivery of vitamins. *Cur. Nanosc*. **5,** 1–14.

Wang, L., Liu, Y., Li, W., Jiang, X., Ji, Y., Wu, X., Xu, L., Qiu, Y., Zhao, K., Wei, T., *et al.* (2011). Selective targeting of gold nanorods at the mitochondria of cancer cells: Implications for cancer therapy. *Nano Lett*. **11,** 772–780.

Weber, T. A., and Reichert, A. S. (2010). Impaired quality control of mitochondria: Aging from a new perspective. *Exp. Gerontol*. **45,** 503–511.

Xiong, S., Li, H., Yu, B., Wu, J., and Lee, R. J. (2010). Triggering liposomal drug release with a lysosomotropic agent. *J. Pharm. Sci*. **99,** 5011–5018.

Zhong, Y., Yingge, Z., Yanlian, Y., Lan, S., Dong, H., Hong, L., and Chen, W. (2010). Pharmacological and toxicological target organelles and safe use of single-walled carbon nanotubes as drug carriers in treating Alzheimer disease. *Nanomedicine* **6,** 427–441.